LETTERS
PUBLISHED ONLINE: 24 NOVEMBER 2013 | DOI: 10.1038/NCLIMATE2060
nature climate change

Continued global warming after CO_2 emissions stoppage

Thomas Lukas Frölicher[1,2]*, Michael Winton[3] and Jorge Louis Sarmiento[2]

Recent studies have suggested that global mean surface temperature would remain approximately constant on multi-century timescales after CO_2 emissions[1–9] are stopped. Here we use Earth system model simulations of such a stoppage to demonstrate that in some models, surface temperature may actually increase on multi-century timescales after an initial century-long decrease. This occurs in spite of a decline in radiative forcing that exceeds the decline in ocean heat uptake—a circumstance that would otherwise be expected to lead to a decline in global temperature. The reason is that the warming effect of decreasing ocean heat uptake together with feedback effects arising in response to the geographic structure of ocean heat uptake[10–12] overcompensates the cooling effect of decreasing atmospheric CO_2 on multi-century timescales. Our study also reveals that equilibrium climate sensitivity estimates based on a widely used method of regressing the Earth's energy imbalance against surface temperature change[13,14] are biased. Uncertainty in the magnitude of the feedback effects associated with the magnitude and geographic distribution of ocean heat uptake therefore contributes substantially to the uncertainty in allowable carbon emissions for a given multi-century warming target.

A large body of studies using simplified climate models[1–4,6–8] and more sophisticated Earth system models[5,9] find that global mean surface temperature stays roughly constant for a couple of centuries at the value attained when carbon emissions are stopped. These studies suggest that the cooling effect of reduction in radiative forcing R due to the decrease in atmospheric CO_2 is roughly balanced by the warming effect of reduction in ocean heat uptake N, such that the difference $R-N$ remains approximately constant[7]. This effect is a consequence of the fact that: the ocean heat and carbon uptake are both controlled in large part by the physical mixing of shallow oceanic waters into the deeper oceans; and under higher atmospheric CO_2, the reduction of the radiative forcing sensitivity to atmospheric CO_2 is roughly compensated by the higher airborne fraction of anthropogenic CO_2. In this paper we show that feedback effects associated with the magnitude and geographical distribution of ocean heat uptake can lead to increasing temperatures, even if the difference $R-N$ decreases.

We performed multi-century simulations using the Geophysical Fluid Dynamics Laboratory Earth System Model[15,16] (GFDL ESM2M) and the National Centre for Atmospheric Research Climate System Model[17,18] (NCAR CSM1; Methods). Both models are forced with a 1,800 GtC pulse so that the atmospheric CO_2 concentration is instantaneously quadrupled from pre-industrial conditions. Both models simulate a rapid atmospheric CO_2 decrease in the first few years after the quadrupling, followed by a slow decline (Fig. 1a). Forty per cent of the initial atmospheric CO_2 perturbation is removed from the atmosphere within 20 years, 60% within 100 years, and 80% within 1,000 years. The land carbon inventories peak after 120 (ESM2M) and 130 years (CSM1), and the ocean is the only carbon sink thereafter (Supplementary Fig. 1).

Figure 1b shows the simulated global mean surface temperature responses (solid lines) to the instantaneous quadrupling of atmospheric CO_2, and estimates of the equilibrium temperature changes (dashed lines) that would occur if the models were in equilibrium with the contemporaneous CO_2 radiative forcing (see Methods for calculation details). The temperature peaks 15–20 years after the CO_2 quadrupling and decreases to 1.5 (ESM2M) and 1.6 K (CSM1) above pre-industrial levels after 100 years. The large initial drop of atmospheric CO_2 and thus radiative forcing (R in Fig. 2a, left axis) in combination with the reduction in ocean heat uptake (N in Fig. 2a, right axis) causes the initial decrease in temperature. The simulated temperature in CSM1 (blue solid line in Fig. 1b) is initially closer to thermal equilibrium with respect to the contemporaneous CO_2 radiative forcing (blue dashed line in Fig. 1b) than in ESM2M (red lines in Fig. 1b), because of the smaller simulated ocean heat uptake in CSM1. This is emphasized in Fig. 1c, which shows the ratio between the simulated temperature and temperature in thermal equilibrium with the contemporaneous CO_2 radiative forcing, the so-called realized warming fraction. The realized global warming fraction after a century is 74% in the CSM1, but only 46% in ESM2M.

After the first hundred years, the simulated temperature responses between the models diverge. The CSM1 simulates a small decrease of −0.06 K until the fifth century (blue solid line in Fig. 1b; fifth column in Table 1), consistent with a previous study[5]. In contrast, the ESM2M simulates a temperature increase of 0.37 K over the same time period (red solid line in Fig. 1b; fifth column in Table 1). After six (ESM2M) and nine (CSM1) hundred years, the system is close to the equilibrium temperature expected from the slowly decreasing atmospheric CO_2 concentration. At this point, ocean heat uptake is near zero (N in Fig. 2a) and temperature (solid lines in Fig. 1b) is approximately the equilibrated temperature (T_{eq}, dashed lines in Fig. 1b) that is given by the ratio of radiative forcing R and equilibrium climate feedback factor λ($T_{eq} = R/\lambda$). The temperature differences between the models at the end of the simulations are due to their different equilibrium climate feedback factors, as intermodel differences in radiative forcings are small. The simulated temperature (red solid line in Fig. 1b) in ESM2M slightly overshoots the estimated equilibrium temperature (red dashed line

[1]Environmental Physics, Institute of Biogeochemistry and Pollutant Dynamics, ETH Zürich, 8092 Zürich, Switzerland, [2]Program in Atmospheric and Oceanic Sciences, Princeton University, Princeton, New Jersey 08544, USA, [3]Geophysical Fluid Dynamics Laboratory, National Oceanic and Atmospheric Administration, Princeton, New Jersey 08542, USA. *e-mail: thomas.froelicher@usys.ethz.ch

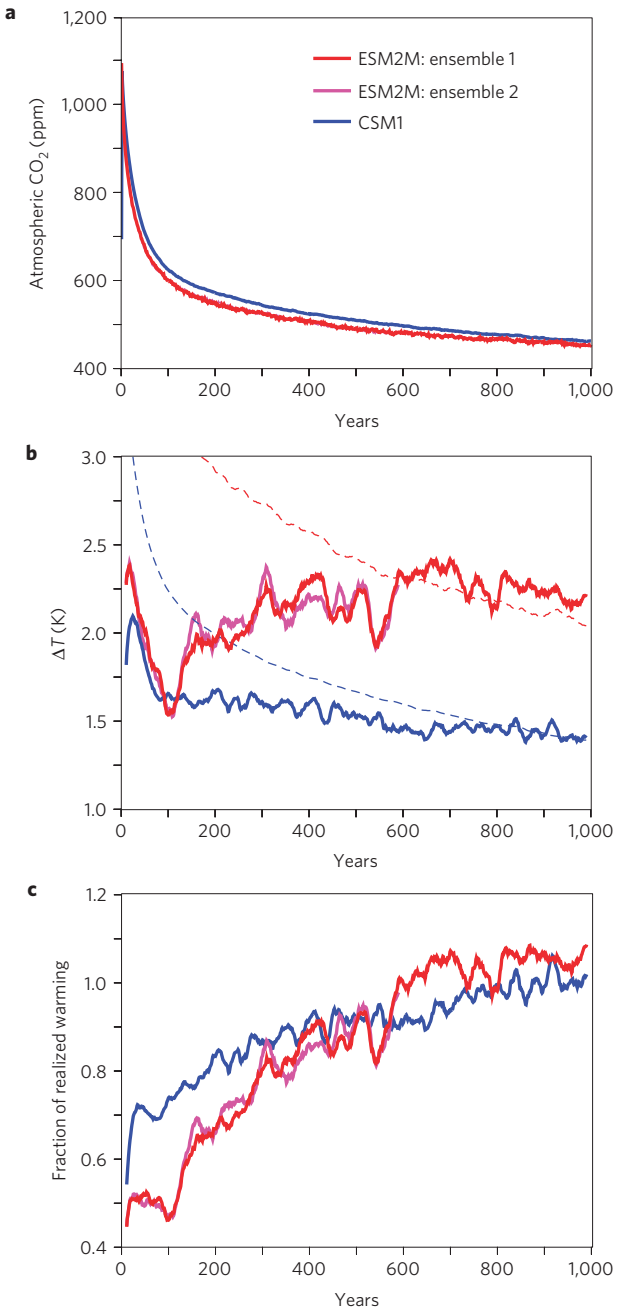

Figure 1 | Idealized carbon dioxide emission scenarios and global mean temperature responses. a–c, Time series of simulated global mean atmospheric CO_2 (**a**), surface temperature changes (**b**) and the ratio of actual and equilibrium temperature after instantaneous quadrupling of the pre-industrial atmospheric CO_2 concentration (**c**). Times series in **b**,**c** have been smoothed with a 20-yr running mean and emphasize the differences between the transient simulations and the pre-industrial control simulations. Legend in **a** applies to all panels. Solid lines in **b** show the simulated temperature responses and dashed lines show the estimated equilibrium temperature responses.

in Fig. 1b) at the end of the simulation as the perturbation ocean heat flux becomes negative (red line for N in Fig. 2a). Thus, the ocean contributes to the warming at the end of the simulation rather than opposing it. It is important to note that we use a simplified expression to estimate the CO_2 radiative forcings (see equation (2)). Thus, the estimated equilibrium temperatures might be slightly different from the 'true' modelled values.

The warming response in ESM2M between the second and fifth century is especially surprising, because the decline in radiative forcing due to the decrease in atmospheric CO_2 exceeds the decline in ocean heat uptake over the this period (decreasing R–N in Fig. 2b). In light of earlier studies and arguments, this is expected to lead to decreasing temperatures in both models. To understand this remarkable behaviour, we make use of the modified standard 'zero-layer' energy balance model of the climate system[10]:

$$\Delta T(t) = \frac{R(t) - \varepsilon N(t)}{\lambda} \quad (1)$$

where ΔT is the global mean surface temperature change, R is the stratospheric-adjusted[19] radiative forcing, λ is the equilibrium climate feedback factor, N is the net radiation flux at the top of the atmosphere (approximately equal to ocean heat uptake on decadal and longer timescales) and ε is the ocean heat uptake efficacy. Ref. 10 showed that ocean heat uptake has a greater global mean surface temperature impact per watt per square metre than the CO_2 radiative forcing, and therefore applied an efficacy factor to the ocean heat uptake. In other words, for the same watt per square metre change in ocean heat uptake and CO_2 radiative forcing, the global mean surface temperature change induced by ocean heat uptake is (generally) larger than that induced by atmospheric CO_2. What causes this efficacy to be greater than 1? As is the case for the efficacy of other forcing agents[19], the ocean heat uptake efficacy is controlled by the relationship between the geographical pattern of ocean heat uptake and the regional climate feedbacks. The low latitudes are generally characterized by strong net negative (stabilizing) feedbacks owing to large negative Planck and lapse rate feedback, whereas the high latitudes feature weak or even positive feedbacks owing to less-negative Planck as well as positive lapse rate, cloud and albedo feedback[11]. Note that there is another way to produce a geographically varying feedback[20] not to be confused with the local definition[11] discussed here. As the ocean heat uptake occurs dominantly at high latitudes it is subject to reduced climate damping relative to geographically broad CO_2 forcing. Ocean heat uptake efficacy may be influenced by regional radiation feedback distribution as well as by ocean circulation changes, because changes in ocean circulation strongly impact the ocean heat uptake and storage pattern[21]. The efficacies of the ESM2M (ensemble 1) and the CSM1 are 1.9 and 1.7, respectively (see equation (3) and Supplementary Table 1 for calculation details).

Table 1 shows the temperature change budget over the period of warming differences (year 100–500). First, the decrease in radiative forcing R scaled by the equilibrium climate feedback factor λ causes a cooling of −0.60 K (ESM2M) and −0.39 K (CSM1; second column in Table 1). Second, the joint effect of the reduction in ocean heat uptake N and amplification of this reduction by the efficacy ε and the equilibrium climate feedback factor λ causes a warming of 0.86 K (ESM2M) and 0.30 K (CSM1) over the same period (third column in Table 1). As a result, the warming effect (0.86 K) due to reduction in ocean heat uptake exceeds the radiative cooling effect (−0.60 K) due to reduction in atmospheric CO_2 and leads to an overall warming of 0.26 K in ESM2M (fourth column in Table 1). In contrast, the CSM1 shows a cooling of −0.09 K as the radiative cooling (−0.39 K) exceeds the ocean heat uptake warming (0.30 K). The estimated multi-century temperature changes of 0.26 K (ESM2M) and −0.09 K (CSM1) are in good agreement with the simulated temperature changes of 0.37 K (ESM2M) and −0.06 K (CSM1). The large differences between the models in $-\varepsilon\Delta N/\lambda$ are mainly caused by differences in ocean heat uptake ($-0.55\,W\,m^{-2}$ in ESM2M versus $-0.34\,W\,m^{-2}$ in CSM1) and equilibrium climate feedback factor ($1.19\,W\,m^{-2}\,K^{-1}$ in ESM2M versus $1.90\,W\,m^{-2}\,K^{-1}$ in CSM1). The small differences in efficacy play a less dominant role here and can explain 20% of total global

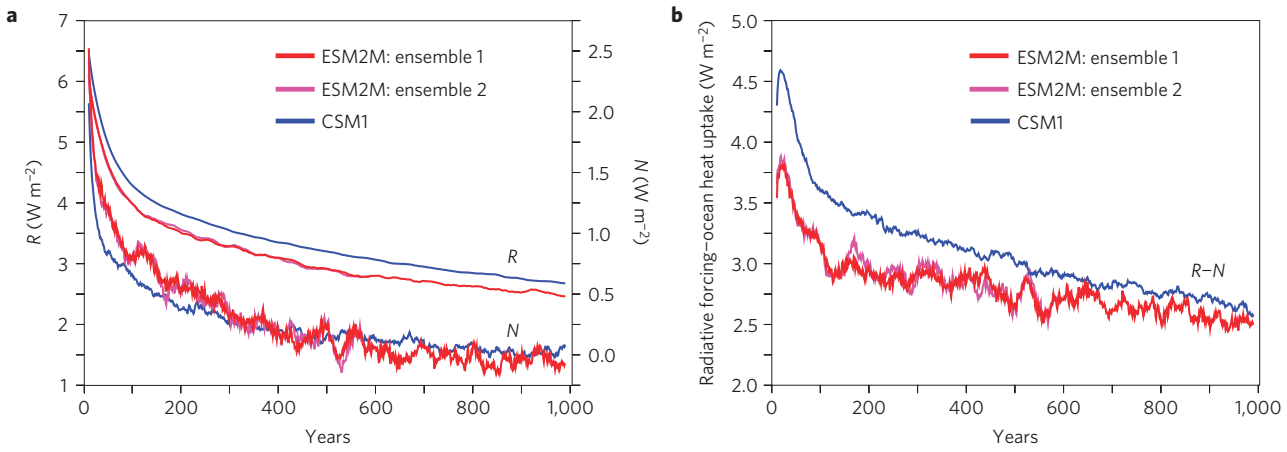

Figure 2 | Simulated changes in ocean heat uptake and radiative forcing. a,**b**, Time series of R (top set of curves) and N (bottom set of curves) (**a**), and R–N (**b**). Times series have been smoothed with a 20-yr running mean. The radiative forcings in both models have been calculated using the simplified expression $R = 5.35 \times \ln(CO_2(t)/CO_2(t=0))$. The estimated radiative forcings of 3.7 W m^{-2} for a doubling of CO_2 using the simplified expression are consistent with the radiative forcings of 3.5 W m^{-2} (ESM2M; ref. 23) and 3.5 W m^{-2} (CSM1; ref. 24) based on radiative transfer code experiments.

Table 1 | Temperature change budget over the period of warming differences.

Model	$\Delta R/\lambda$ (radiative cooling effect)	$-\varepsilon\Delta N/\lambda$ (the ocean warming effect)	$\Delta R/\lambda - \varepsilon\Delta N/\lambda$ (estimated temp change)	ΔT (actual temp change)
ESM2M	−0.60	0.86	0.26	0.37
CSM1	−0.39	0.30	−0.09	−0.06
ESM2M–CSM1	−0.21	0.56	0.37	0.31

The estimated temperature changes calculated from $\Delta R/\lambda$, $-\varepsilon\Delta N/\lambda$ and $\Delta R/\lambda - \Delta\varepsilon N/\lambda$, and actual simulated temperature changes over the period of warming difference between the second (average over the period 101–200) and fifth (average over the period 401–500) century for the two models and their differences. Units are in kelvin. Changes in radiative forcing R are −0.71 W m^{-2} (ESM2M) and −0.74 W m^{-2} (CSM1), and changes in ocean heat uptake N are −0.55 W m^{-2} (ESM2M) and −0.34 W m^{-2} (CSM1), respectively. Values for ε and λ are taken from Supplementary Table 1.

warming differences between the models. Note that equation (1) does not work well in the first century of the simulation as ocean heat uptake efficacy increases with time during this adjustment period, and for short-term variations as interannual variations in ocean heat uptake are not concentrated in high latitudes and are probably associated with El Niño/Southern Oscillation variability.

Recent studies suggest that efficacy evaluated at the time of doubling in 1% CO_2 increase experiments is very variable between climate models[10,12], but generally greater than unity with a median value of 1.3, and values as large as 2. The wide range of possible efficacy values together with changes in the total ocean heat uptake can therefore contribute substantially to uncertainties in the short-term and multi-century warming response for a given carbon emission pulse (Supplementary Fig. 2). Even the sign of change is unclear on multi-century timescales. An efficacy closer to unity, for example, would lead to decreasing temperatures in both models between the second and fifth century (Supplementary Fig. 2) as the difference between radiative forcing and ocean heat uptake decreases in both models (Fig. 2b).

The importance of the ocean heat uptake efficacy also becomes apparent when estimating the equilibrium climate sensitivity T_{eq} $(2 \times CO_2)$ (the equilibrium global surface temperature response to doubling of CO_2; see Methods). A widely used extrapolation approach to diagnose T_{eq} $(2 \times CO_2)$ (herein referred to as the 'Gregory method') uses 150 years of ocean heat uptake and surface temperature data from an abrupt CO_2 quadrupling experiment, where atmospheric CO_2 is prescribed at $4 \times CO_2$ (refs 13,14). The Gregory T_{eq} $(2 \times CO_2)$ estimate of 2.4 K for ESM2M is much smaller than the T_{eq} $(2 \times CO_2)$ estimate of 3.1 K calculated from our carbon pulse experiments because the Gregory method does not adequately assess the approach to equilibrium along high-efficacy trajectories[11,22] (Supplementary Fig. 3a). The Gregory T_{eq} $(2 \times CO_2)$ for CSM1 is in agreement with our carbon pulse T_{eq} $(2 \times CO_2)$, but the Gregory method largely underestimates the radiative forcing for a doubling of CO_2 in CSM1 because of nonlinear adjustment in the first couple of years (Supplementary Fig. 3b). It is both the shortness of the experiment and the inclusion of the early adjustment in the linear estimate that cause problems for the Gregory method (see Supplementary Text for detailed discussion). As an alternative, we propose to use our carbon pulse simulation experiments with freely evolving atmospheric CO_2 to calculate the T_{eq} $(2 \times CO_2)$, because: the pulse experiment is more relevant to the actual adjustment that will occur following CO_2 emissions than the step CO_2 experiments used at present[13,14]; the T_{eq} $(2 \times CO_2)$ obtained from our carbon pulse experiments of 3.1 K (ESM2M) and 2.0 K (CSM1) for a doubling of CO_2 are in good agreement with the T_{eq} $(2 \times CO_2)$ estimates of 3.4 K (ESM2M; ref. 23) and 2.1 K (CSM1; ref. 24) using atmosphere/slab–ocean configurations of the same models; and the costs to run the simulations are significantly less than running a coupled model to equilibrium under constant radiative forcing. The impulse response function of atmospheric CO_2 from our experiments can be used in atmosphere–ocean coupled general circulation models that do not include carbon cycle components as a forcing to run the same pulse simulations (Supplementary Table 2).

A present study using global ocean heat uptake, atmospheric temperature and radiative forcing data from most recent climate observations suggests a relatively small transient climate response of 1.3 K (0.9–2.0 K) and a small equilibrium climate sensitivity of 2.0 K (1.2–3.9 K; ref. 25; Supplementary Fig. 3c and Text for extended

discussion). Our study suggests, however, that small transient climate responses do not necessarily imply small equilibrium climate sensitivities, because of non-unity efficacy (Supplementary Fig. 3c). ESM2M simulates a transient climate response of 1.5 K, which is close to the observational-based estimate of 1.3 K, but the simulated equilibrium climate sensitivity of 3.1 K is much larger than the observational-based estimate of 2.0 K. If the real world were to behave in a similar manner as ESM2M then only a small fraction of the total warming due to past carbon emissions has thus far been realized.

Recent research has suggested that the magnitude of CO_2-induced warming that will occur and persist for the coming centuries is mainly determined by the amount of future cumulative carbon emissions and that past emissions commit us to hundreds of years at approximately the level of CO_2-induced warming that has already been realized. Thus, cumulative carbon emissions are a powerful metric for climate stabilization levels and thus policy, as only the warming per unit cumulative emissions is needed to make projections of global temperature on multi-centennial timescales[1,6,26]. Our study shows that global mean temperature may even increase after zero carbon emissions, because of feedback effects arising in response to the magnitude and geographic structure of ocean heat uptake. Thus, estimates of allowable carbon emissions required to remain below the 2 °C global warming target may be significantly lower than previously thought. A better understanding and monitoring of how ocean circulation changes impact regional ocean heat uptake and thus efficacy is necessary to narrow uncertainties in climate change projections.

Methods

Models. We performed simulations with two different fully coupled carbon cycle–climate models, GFDL ESM2M and NCAR CSM1. Both models include representations of the physical climate system as well as ocean and land biogeochemistry. Atmospheric CO_2 is treated as a prognostic variable in both models. The ESM2M has an oceanic horizontal resolution of approximately $1° \times 1°$ and 50 vertical levels, and the CSM1 has an oceanic horizontal resolution of approximately $3.5° \times 3.5°$ and 25 vertical levels.

Simulations. The two-member ensemble simulation (1,000- and 600-yr long) with the ESM2M model is forced with a carbon pulse of 1,800 GtC so that the atmospheric CO_2 concentration is instantaneously quadrupled from pre-industrial conditions in the first time step of the simulation. The single 1,000-yr long simulation with the CSM1 is forced with the same amount of carbon emissions, but the pulse is distributed over the first year of the simulation. For comparison, humankind released 365 ± 30 GtC fossil fuel and cement emissions between 1750 and 2011 (ref. 27), with an additional 190 ± 80 GtC due to land use change[28]. Non-CO_2 forcing agents are kept constant at pre-industrial levels in all simulations. Corresponding 1,000-yr (ESM2M) and 479-yr (CSM1) pre-industrial control simulations are used to correct for model drift. The idealized pulse scenarios give virtually identical long-term temperature changes as when using the same amount of cumulative carbon emissions following more 'realistic' emission trajectories[4].

Calculation of stratospheric-adjusted radiative forcing, efficacy and equilibrium climate sensitivity from the carbon pulse experiment. The expression radiative forcing (denoted by R) is commonly used in characterizing anthropogenic perturbations in the radiative energy budget of the Earth's climate system. Here, such a perturbation is the change in atmospheric CO_2 concentration. Specifically, the stratospheric-adjusted radiative forcing is the change in net irradiance at the tropopause after allowing for stratospheric temperatures to readjust to radiative equilibrium, but with surface and tropospheric temperatures and state held fixed at the unperturbed values[19]. The radiative forcing is calculated using the simplified expression[29]:

$$R(t) = 5.35 \ln \frac{CO_2(t)}{CO_2\ (t=0)} \quad (2)$$

To calculate the efficacy and the equilibrium climate feedback factor, we use the modified standard 'zero-layer' energy balance model of the climate system[10]:

$$\Delta T(t) = \frac{1}{\lambda} R(t) - \frac{\varepsilon}{\lambda} N(t) \quad (3)$$

By applying a multiple linear regression of simulated centennial-averaged temperature ΔT on simulated centennial-averaged radiative forcing R and ocean heat uptake N with no intercept, we calculate the efficacy (ε) and equilibrium climate feedback parameter (λ). The equilibrium climate sensitivity T_{eq} for a doubling of CO_2 is then calculated with $T_{eq}\ (2 \times CO_2) = R_{2\times CO_2}/\lambda$. Values are given in Supplementary Table 1. The concept of efficacy is illustrated in Supplementary Fig. 4.

Received 14 August 2013; accepted 29 October 2013; published online 24 November 2013

References

1. Allen, M. R. *et al.* Warming caused by cumulative carbon emissions towards the trillionth tonne. *Nature* **458,** 1163–1166 (2009).
2. Matthews, H. D. & Caldeira, K. Stabilizing climate requires near-zero emissions. *Geophys. Res. Lett.* **35,** L04705 (2008).
3. Plattner, G-K. *et al.* Long-term climate commitments projected with climate–carbon cycle models. *J. Clim.* **21,** 2721–2751 (2008).
4. Eby, M. *et al.* Lifetime of anthropogenic climate change: Millennial time-scales of potential CO_2 and surface temperature perturbations. *J. Clim.* **22,** 2501–2511 (2009).
5. Frölicher, T. L. & Joos, F. Reversible and irreversible impacts of greenhouse gas emissions in multi-century projections with the NCAR global coupled carbon cycle-climate model. *Clim. Dynam.* **35,** 1439–1459 (2010).
6. Matthews, H. D., Gillet, N., Scott, P. A. & Zickfeld, K. The proportionality of global warming to cumulative carbon emissions. *Nature* **459,** 829–832 (2009).
7. Solomon, S., Plattner, G-K., Knutti, R. & Friedlingstein, P. Irreversible climate change due to carbon dioxide emissions. *Proc. Natl Acad. Sci. USA* **106,** 1704–1709 (2009).
8. Zickfeld, K., Eby, M., Matthews, H. D. & Weaver, A. J. Setting cumulative emissions targets to reduce the risk of dangerous climate change. *Proc. Natl Acad. Sci. USA* **106,** 16129–16134 (2009).
9. Gillet, N. P., Arora, V. K., Zickfeld, K., Marshal, S. J. & Merryfield, W. J. Ongoing climate change following a complete cessation of carbon dioxide emissions. *Nature Geosci.* **4,** 83–87 (2011).
10. Winton, M., Takahashi, K. & Held, I. M. Importance of ocean heat uptake efficacy to transient climate change. *J. Clim.* **23,** 2333–2344 (2010).
11. Armour, K. C., Bitz, C. M. & Roe, G. H. Time-varying climate sensitivity from regional feedbacks. *J. Clim.* **26,** 4518–4534 (2013).
12. Geoffroy, O. *et al.* Transient climate response in a two-layer energy-balance model. Part II: Representation of the efficacy of deep-ocean heat uptake and validation for CMIP5 AOGCMs. *J. Clim.* **26,** 1859–1879 (2013).
13. Gregory, J. M. *et al.* A new method for diagnosing radiative forcing and climate sensitivity. *Geophys. Res. Lett.* **31,** L03205 (2004).
14. Andrews, T., Gregory, J. M., Webb, M. J. & Taylor, K. E. Forcing, feedbacks and climate sensitivity in CMIP5 coupled atmosphere-ocean climate models. *Geophys. Res. Lett.* **39,** L09712 (2012).
15. Dunne, J. P. *et al.* GFDL's ESM2 global coupled climate-carbon Earth system models. Part I: Physical formulation and baseline simulation characteristics. *J. Clim.* **25,** 6646–6665 (2012).
16. Dunne, J. P. *et al.* GFDL's ESM2 global coupled climate-carbon Earth system models. Part II: Carbon system formulation and baseline simulation characteristics. *J. Clim.* **26,** 2247–2267 (2013).
17. Doney, S. C., Lindsay, K., Fung, I. & John, J. Natural variability in a stable 1000-yr global coupled climate-carbon cycle simulation. *J. Clim.* **19,** 3033–3054 (2006).
18. Frölicher, T. L., Joos, F., Plattner, G-K., Steinacher, M. & Doney, S. C. Natural variability and anthropogenic trends in oceanic oxygen in a coupled carbon cycle-climate model ensemble. *Glob. Biogeochem. Cycle* **23,** GB1003 (2009).
19. Hansen, J. *et al.* Efficacy of climate forcings. *J. Geophys. Res.* **110,** D18104 (2005).
20. Zelinka, M. D. & Hartmann, D. L. Climate feedbacks and their implications for poleward energy flux changes in a warming climate. *J. Clim.* **25,** 608–624 (2012).
21. Winton, M., Griffies, S. M., Samuels, B. L., Sarmiento, J. L. & Frölicher, T. L. Connecting changing ocean circulation with changing climate. *J. Clim.* **26,** 2268–2278 (2013).
22. Li, C., von Storch, J-S. & Marotzke, J. Deep-ocean heat uptake and equilibrium climate response. *Clim. Dynam.* **40,** 1017–1086 (2013).
23. Delworth, T. L. *et al.* GFDL's CM2 global coupled climate models. Part I: Formulation and simulation characteristics. *J. Clim.* **19,** 643–674 (2006).
24. Meehl, G. A. *et al.* Response of the NCAR climate system model to increased CO_2 and the role of physical processes. *J. Clim.* **13,** 1879–1898 (2000).
25. Otto, A. *et al.* Energy budget constraints on climate response. *Nature Geosci.* **6,** 415–416 (2013).
26. Matthews, H. D., Solomon, S. & Pierrehumbert, R. Cumulative carbon as a policy framework for achieving climate stabilization. *Phil. Trans. R. Soc. A* **370,** 4365–4379 (2012).

27. Boden, T., Marland, G. & Andres, R. J. *Global, Regional, and National Fossil-Fuel* CO_2 *Emissions* (Carbon Dioxide Information Analysis Center, Oak Ridge National Laboratory, US Department of Energy, 2011); http://dx.doi.org/10.3334/CDIAC/00001_V2010
28. Houghton, R. A. *et al*. Carbon emissions from land use and land-cover change. *Biogeosciences* **9,** 5125–5142 (2012).
29. Ramaswamy, V. *et al*. in *IPCC Climate Change 2001: The Scientific Basis* (ed. Houghton, H. T.) 349–416 (Cambridge Univ. Press, 2001).

Acknowledgements

We thank D. Paynter, T. Merlis, K. Rodgers, J. Dunne and N. Gruber for useful discussions and comments. We also thank B. L. Samuels for conducting the GFDL ESM2M simulations and R. Roth for help with the impulse response function calculations. Simulations with the NCAR CSM1 were carried out at the University of Bern, Switzerland. T.L.F. acknowledges financial support from the SNSF (Ambizione grant PZ00P2_142573). J.L.S. was supported by the Carbon Mitigation Initiative (CMI) project at Princeton University, sponsored by BP.

Author contributions

T.L.F. and M.W. designed the study and undertook main analysis. T.L.F. performed simulations and wrote the paper, with significant text supplied by all authors, who also discussed the results.

Additional information

Supplementary information is available in the online version of the paper. Reprints and permissions information is available online at www.nature.com/reprints. Correspondence and requests for materials should be addressed to T.L.F.

Competing financial interests

The authors declare no competing financial interests.